The zero-energy state in graphene in a high magnetic field

Joseph G. Checkelsky, Lu Li and N. P. Ong
Department of Physics, Princeton University, Princeton, NJ 08544, USA
(Dated: February 1, 2008)

The fate of the charge-neutral Dirac point in graphene in a high magnetic field H has been investigated at low temperatures ($T \sim 0.3$ K). In samples with small gate-voltage offset V_0, the resistance R_0 at the Dirac point diverges steeply with H, signalling a crossover to an insulating state in high field. The approach to the insulating state is highly unusual. Despite the steep divergence in R_0, the profile of R_0 vs. T in fixed H saturates to a T-independent value below 2 K, consistent with gapless charge-carrying excitations.

PACS numbers: 73.63.-b,73.21.-b,73.43.-f

The discovery of the quantum Hall effect (QHE) in monolayer graphene crystals provides a new system for investigating relativistic Dirac-like excitations in solids [1, 2, 3, 4, 5, 6]. In a magnetic field H, the system forms Landau Levels (indexed by n) that are 4-fold degenerate. The Hall conductivity σ_{xy} is accurately quantized as the chemical potential μ is changed from the hole part to electron part of the Dirac spectrum. Considerable attention has focussed on the $n = 0$ Landau Level (LL), especially on the nature of the electronic state at the charge-neutral point ($\mu = 0$) in an intense magnetic field H. Several groups [7, 8, 9, 10, 11, 12] have predicted that a large field stabilizes the quantum Hall ferromagnetic (QHF) state, in which the pseudospins describing the valley degree of freedom become ferromagnetically ordered. In a second group of theories [13, 14], interaction causes an excitonic gap to open at the Dirac point. Experiments are actively addressing these issues [15, 16, 17]. Jiang *et al.* [16] have inferred that the sublevel gaps at $\nu = 0$ and ± 1 arise from lifting of the spin and sub-lattice degeneracies, respectively, and inferred a many-body origin for the states. We have found that, in samples with small V_0 (the gate voltage needed to align μ with the Dirac point), the value R_0 of the resistance R_{xx} at the Dirac point diverges steeply with H, i.e. a large H drives the Dirac point insulating. Despite the strong H dependence, R_0 saturates to a T-independent value below 2 K, providing evidence for charged, gapless excitations. In samples with large V_0, this divergence in R_0 is shifted to higher fields.

Following Refs. [1, 2, 4], we peeled single-layer graphene crystals (3-10 μm in length) from Kish graphite on a Si-SiO_2 wafer. Au/Cr contacts were deposited using e-beam lithography (Fig. 1a, inset). We have found that the high-field behavior of R_0 is strongly correlated with V_0 (Table I). All samples (except K22) have μ lying in the electron band (positive V_0). Samples in which $|V_0| < 1$ V (K7 and K22) display a very large $R_0(14)$ (resistance measured at 14 T and 0.3 K), which arises from the strong divergence mentioned. By contrast, in samples with large $|V_0|$, $R_0(14) \leq 7$ kΩ.

Figure 1a shows the variation of R_{xx} in K7 plotted vs. the shifted gate voltage $V_g' = V_g - V_0$ with H held at 8, 11 and 14 T (at $T = 0.3$ K). The striking feature here is that the peak corresponding to the $n = 0$ LL increases to >100 kΩ at 14 T, whereas the peaks corresponding to $n = \pm 1$ remain below ~7 kΩ. As in Refs. [1, 2, 3, 4, 5], the Hall conductivity σ_{xy} (Panel b) displays plateaus given by [12]

$$\sigma_{xy} = \frac{\nu e^2}{h} = \frac{4e^2}{h}\left(n + \frac{1}{2}\right), \qquad (1)$$

where n indexes the 4-fold degenerate LL and ν indexes individual sublevels. In K7, the 'zero' plateau $\sigma_{xy} \simeq 0$ at $V_g' = 0$ is already visible at $H = 8$ T.

Narrowing our focus to the $n = 0$ LL, we examine R_{xx} in the $n = 0$ LL as a function of T, with H fixed at 14 T (Fig. 2a). We see that, from 40 to 0.3 K, R_0 rises steeply from 4 kΩ to 190 kΩ. The curve of the conductivity σ_{xx} plotted vs. V_g' reveals a 2-peak structure that implies splitting of the 4-fold degeneracy by a gap Δ (Fig. 2b). At 100 K, the two peaks are already resolved. With decreasing T, the minimum at $V_g' = 0$ initially deepens rapidly, but saturates below ~2 K. The Hall conductivity σ_{xy} at 0.3 K (thin curve) displays a well-defined plateau on which $\sigma_{xy} \simeq 0$. Because the next plateau is at $\sigma_{xy} = 2(e^2/h)$, we infer that each of the peaks in σ_{xx} is comprised of 2 unresolved sublevels. The opening of the gap causes σ_{xx} (at $V_g' = 0$) to fall rapidly with decreasing T, until saturation occurs below 2 K.

The behavior of R_0 described here is qualitatively different from that in, for e.g., Ref. [15]. To understand the difference, we have examined several samples (Table I). As mentioned, the offset gate V_0 is a crucial parameter. Figure 2c compares the curves of R_{xx} ($n = 0$ LL) in the

Sample	V_0(V)	$R_0(14)$(kΩ)	μ_e(1/T)
K5	3	80	0.3
K7	1	190	1.3
K8	12	15	0.6
K18	20	7.5	0.9
K22	-0.6	>280	2.5
K29	22.5	7	0.2

TABLE I: Sample parameters. V_0 is the gate voltage needed to bring μ to 0. $R_0(14)$ is R_0 measured at $H = 14$ T and $T = 0.3$ K. μ_e is the electron mobility at $H = 0$.

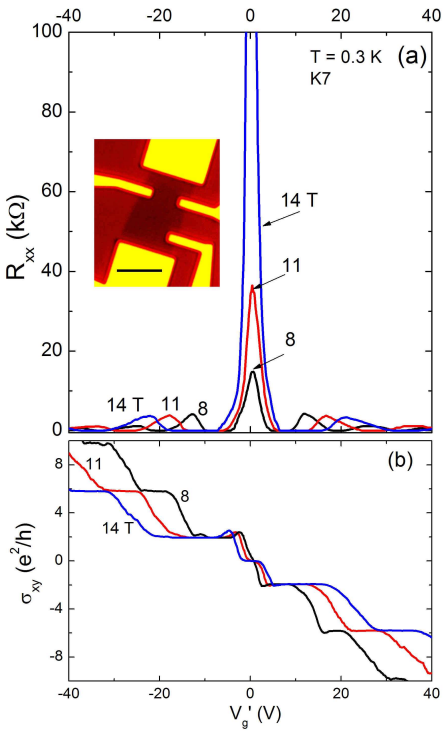

FIG. 1: (color online) The resistance R_{xx} (Panel a) and Hall conductivity σ_{xy} (b) in Sample K7 versus (shifted) gate voltage $V_g' = V_g - V_0$ at 0.3 K with H fixed at 8, 11 and 14 T. Peaks of R_{xx} at finite V_g' correspond to the filling of the $n = 1$ and $n = 2$ LLs. At $V_g' = 0$, the peak in R_{xx} grows to 190 kΩ at 14 T. The inset shows in false color a graphene crystal (dark red) with Au leads deposited (yellow regions). The bar indicates 5 μm. Panel b shows the quantization of σ_{xy} at the values $(4e^2/h)(n+\frac{1}{2})$. At 0.3 K, $\sigma_{xy} = 0$ in a a 2-Volt interval around $V_g' = 0$.

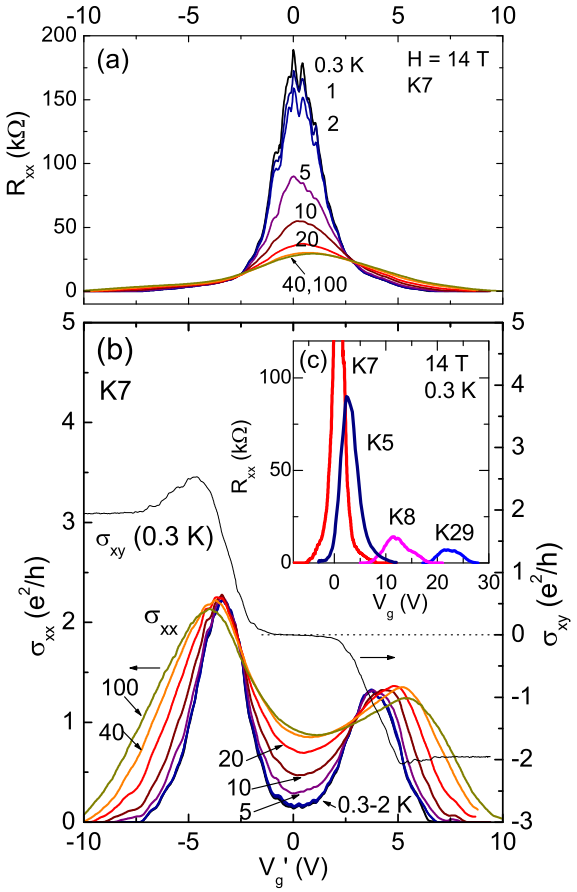

FIG. 2: (color online) The resistance R_{xx}, conductivity σ_{xx} and the Hall conductivity σ_{xy} in K7 vs. the shifted gate voltage V_g', with H fixed at 14 T. As T decreases to 0.3 K, the zero-energy peak in R_{xx} (Panel a) rises steeply to 190 kΩ. Panel (b) shows that, as T decreases, double peaks in σ_{xx} are clearly resolved. Between the peaks, σ_{xx} falls rapidly but saturates below 2 K. The Hall conductivity at 0.3 K (thin curve) displays a clear plateau ($|\sigma_{xy}| < 0.02e^2/h$) in the interval $-1V < V_g' < 1V$. Panel (c) compares R_{xx} (of $n = 0$ LL) vs. unshifted gate V_g in the samples K5, K7, K8 and K29 at 0.3 K. In each sample, R_{xx} peaks at V_0. As V_0 increases, $R_0(14)$ rapidly decreases.

samples K5, K7, K8 and K29, all measured at 14 T at $T = 0.3$ K. For each sample, we have plotted R_{xx} vs. the unshifted gate voltage V_g, so its peak automatically locates V_0. It is clear that K7 ($V_0 = 1$ V) has the highest peak, followed by K5 ($V_0 = 3$ V), whereas K8 ($V_0 = 12$ V) and K29 (22.5 V) have peaks that are severely suppressed. Further insight into this pattern of suppression is given below when we examine the H dependence of R_0 at low T.

Sample self-heating may also obscure the divergence. We find that, below 1 K, self-heating becomes serious when the dissipation exceeds ∼2 pW. The measurements of R_{xx} vs. V_g were repeated at 3 currents (I= 0.6, 2 and 15 nA) at $T = 0.3$ K. The results at $I = 0.6$ and 2 nA are virtually identical. However, the curve at 15 nA is 30% smaller near $V_g' = 0$, consistent with heating. Hence, we have kept I at 2 nA to eliminate self-heating as a problem. Heating at the contacts is negligible because of the small contact resistances (∼1 kΩ) relative to R_0.

Hereafter, we focus on R_0, or equivalently, the Dirac-point conductivity $\sigma_{xx}^0 \equiv L/wR_0$ (L and w are the length and width). Curves of the conductivity versus $\log_{10} T$ are shown in Fig. 3a at selected fields. In low fields ($H <$ 9 T), the T dependence of σ_{xx}^0 is quite mild. As H is increased to 14 T, the opening of the gap Δ (between the n=0 sublevels) causes the conductance to decrease sharply below 40 K. However, instead of falling to 0, σ_{xx}^0 saturates below 2 K to a T-independent residual value σ_{res}, as anticipated in the discussion of Fig. 2b. The existence of this residual σ_{res}, which is highly sensitive to H, is one of our key findings.

The field dependence of σ_{res} is best viewed as a divergent R_0. Figure 3b shows the rising profile of R_0 vs. H

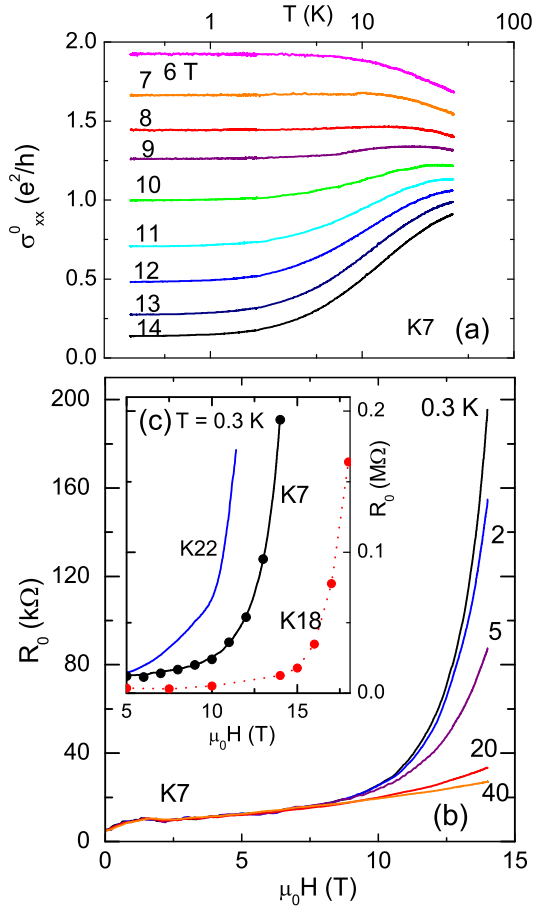

FIG. 3: (color online) The T dependence of σ^0_{xx} in K7 (= L/wR_0) and the H dependence of R_0 at low temperature. Panel a shows curves of σ^0_{xx} vs. $\log_{10}T$ with H fixed at 6-14 T. For $H > 8$ T, the gap Δ causes σ^0_{xx} to decrease markedly until saturation at the residual value σ_{res} occurs below 2 K. Panel (b) displays the steep increase in R_0 vs. H in K7 at selected T. At 0.3 K, R_0 appears to diverge at a field near 18 T (see Fig. 4b). Panel (c) compares the $R_0(H)$ profiles in Samples K7, K18 and K22. In Sample K18 (V_0 = 20 V), the divergence in R_0 becomes apparent only above 14 T, whereas in K22 (V_0 = -0.6 V) R_0 starts to diverge at fields lower than in K7. In K7, we have plotted R_0 values measured by sweeping V_g at fixed H (solid symbols) with R_0 measured by sweeping H with V_g' fixed at 0 (solid curve), to show consistency.

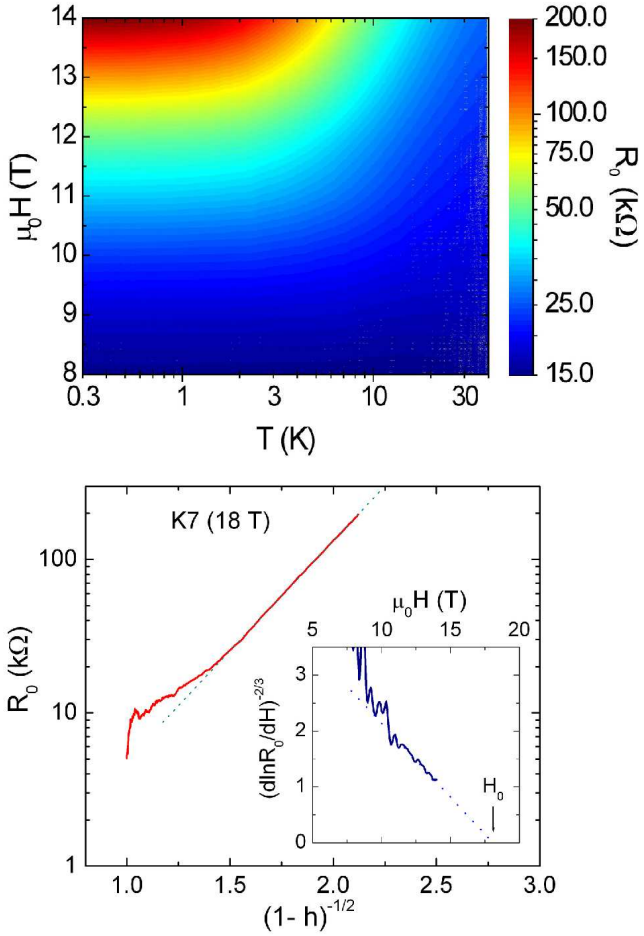

FIG. 4: (color online) (Panel a) The contour plot of $R_0(T, H)$ (K7) in the T-H plane (vertical bar shows values of R_0). The contour lines emphasize the unusual approach to the insulating state. At low T, R_0 is unchanged on a horizontal path (H held fixed), but it rises rapidly on a vertical path (increasing H at fixed T). Panel (b) displays $\log R_0$ vs. $1/\sqrt{1-h}$ in K7 at T = 0.3 K, with $h = H/H_0$, where H_0 = 18 T. The linear segment at large R_0 shows that the divergence is consistent with $R_0(h) \sim \exp[2b/\sqrt{1-h}]$ with $b \sim$0.7. In Panel (c), the plot of $(d \ln R_0/dH)^{-2/3}$ vs. H shows a high-field linear segment that extrapolates to zero at $\sim H_0$ (18 T).

in sample K7 at selected temperatures. The divergent form at the lowest T (0.3 K) strongly suggests that the system is rapidly approaching a field-induced crossover (or transition) to an insulating state.

In light of the importance of V_0, it is instructive to see how the profile of R_0 vs. H varies between samples. Figure 3c compares the results in K7, K18 and K22 at T = 0.3 K. In K18, where V_0 (20 V) is quite large, the divergence in $R_0(H)$ becomes noticeable only in fields above 14 T. Conversely, in K22 for which V_0 (-0.6 V) is slightly smaller than in K7, R_0 diverges at field scales smaller than in K7. From the trend, it is clear that the divergence in R_0 is shifted to ever higher fields as V_0 increases. Referring back to Fig. 2c, we now see that the strong suppression of $R_0(14)$ in samples with large V_0 simply reflects the shift of the divergence to larger H. These results underscore the importance of choosing samples with $|V_0| < 1$ V for investigating the intrinsic properties of the Dirac-point. In the case of K7, we have also checked that the 2 procedures for measuring R_0 (varying V_g at fixed H or vice versa) give consistent values.

The variation of $R_0(T, H)$ in K7 is conveniently represented in a contour plot in the T-H plane (Fig. 4).

Below ∼2 K, the contour lines are horizontal, which implies that R_0 is unchanged if the sample is cooled in fixed H. This provides evidence that σ_{res} involves gapless excitations. However, if T is fixed, R_0 rises steeply with H, implying proximity to the insulating state (deep-red region). When a system approaches the insulating state, its resistivity generally diverges as $T \to 0$, as a result of either strong localization (variable-range hopping) or the opening of a mobility gap (weak localization is not relevant here because of the intense H). In both cases, decreasing T reduces the conductance because the itinerant states are severely depopulated. Hence, the pattern in Fig. 4a is most unusual. The gaplessness of σ_{res} suggests that, below 2 K, these excitations are protected from the effects of changing T. Paradoxically, they are not protected from an increasing H, which reduces the current carried at an exponential rate.

In the theory in Refs. [15, 18], the current at the Dirac point is carried by a pair of edge states. The change in R_{xx} vs. H is interpreted as an increased scattering rate as the edge states are pushed closer to the edge.

In samples with small V_0, however, the steep increase in R_0 to ∼200 kΩ (Fig. 3b) suggests a different regime in which Coulomb exchange may be the dominant energy scale. From Figs. 3b and 4a, we infer that R_0 appears to be diverging towards an insulating state in high fields. These considerations lead us to quantify the divergence in R_0.

We find that R_0 fits very well to the form $R_0 \sim \xi(h)^2$, where the correlation length ξ has the Kosterlitz-Thouless (KT) form

$$\xi_{KT} \sim \exp(b/\sqrt{1-h}), \quad (h = H/H_0), \qquad (2)$$

with H replacing T. Plotting $\ln R_0$ vs. $\sqrt{1-h}$, we find that the high-field portion becomes linear (Fig. 4b) when H_0 is adjusted to be 17-18 T. From the slope, we find that the parameter b has the value ∼0.7, in agreement with simulations of the KT transition. For self consistency, we may also let the data determine H_0 by linear extrapolation. By Eq. 2, we have $d\ln R_0/dH \sim (H_0 - H)^{-3/2}$. Hence a plot of $(d\ln R_0/dH)^{-2/3}$ vs. H should cross the H-axis at H_0. Indeed, this quantity, plotted in Fig. 4c, becomes linear at large H and extrapolates to zero at ∼18 T in agreement with (b).

Although consistency with Eq. 2 alone does not prove that a KT transition occurs at H_0, the fit does reveal the striking exponential character of the divergence in R_0. We adopt as a working hypothesis that this reflects the approach to a KT transition. The ordered state at large H is destroyed by the spontaneous appearance of defects which increase exponentially in density at H_0. The steep fall of R_0 below H_0 may reflect the current carried by these defects.

In both the QHF state [7, 8, 9, 10, 11] and the exciton-gap state [13, 14], the 4-fold degeneracy in the $n = 0$ LL is completely lifted in large H to produce an insulator. In the QHF, the starting symmetry is $SU(4)$ if we treat the spin and pseudospin degrees on equal footing [9]. The reduction of the $SU(4)$ to lower symmetries by the effects of Zeeman energy, disorder or lattice discretization is discussed in Refs. [8, 10, 11, 12]. According to Ref. [11] random disorder may force the pseudospins into the plane. If the ordered state indeed has $U(1)$ symmetry, the XY order is susceptible to a KT transition [7, 11]. It would be very interesting to relate the fit of R_0 to Eq. 2 with charged, topological excitations envisioned in the KT transition. Measurements are in progress at higher H to provide further evidence for a transition to the insulating state and to clarify its nature.

We acknowledge valuable discussions with Kun Yang, P. A. Lee, M. Lee, A. Geim and A. Pasupathy. We are indebted to Philip Kim for generously providing Kish graphite crystals. This research is supported by NSF-MRSEC under Grant DMR 0213706, and by the Princeton Center for Complex Materials. Some data were taken in the National High Magnetic Field Lab., Tallahassee, which is supported by NSF and the State of Florida.

[1] K. S. Novoselov *et al.* Science **306**, 666-669 (2004).
[2] K. S. Novoselov *et al.* Proc. Natl. Acad. Sci. USA **102**, 10451-10453 (2005).
[3] K. S. Novoselov *et al.* Nature **438**, 197-200 (2005).
[4] Y. Zhang, J. Tan, H. L. Stormer and P. Kim, Nature **438**, 201-204 (2005).
[5] Y. Zhang *et al.* Phys. Rev. Lett. **96**, 136806 (2006).
[6] Y.-W. Tan *et al.* cond-mat/0707.1807 (2007).
[7] K. Nomura and A. H. MacDonald, Phys. Rev. Lett. **96**, 256602 (2006).
[8] J. Alicea and M. P. A. Fisher, Phys. Rev. B **74**, 075422 (2006).
[9] Kun Yang, S. Das Sarma and A. H. MacDonald, Phys. Rev. B **74**, 075423 (2006).
[10] M. O. Goerbig, R. Moessner and B. Douçot, Phys. Rev. B **74**, 161407(R) (2006).
[11] D. A. Abanin, P. A. Lee and L. S. Levitov, Phys. Rev. Lett. **98**, 156801 (2007).
[12] For a review, see Kun Yang, Solid State Commun. **143**, 27 (2007).
[13] D. V. Khveshchenko, Phys. Rev. Lett. **87**, 206401 (2001).
[14] V. P. Gusynin, V. A. Miransky, S. G. Sharapov, and I. A. Shovkovy, Phys. Rev. B **74**, 195429 (2006).
[15] D. A. Abanin *et al.* Phys. Rev. Lett. **98**, 196806 (2007).
[16] Z. Jiang, Y. Zhang, H. L. Stormer and P. Kim, Phys. Rev. Lett. **99**, 106802 (2007).
[17] Sungjae Cho and Michael S. Fuhrer, cond-mat arXiv:0705.3239v2
[18] D. A. Abanin, P. A. Lee and L. S. Levitov, Phys. Rev. Lett. **96**, 176803 (2006).